Biochimica et Biophysica Acta 1850 (2015) 878–888

Contents lists available at ScienceDirect

Biochimica et Biophysica Acta

journal homepage: www.elsevier.com/locate/bbagen

Review

Towards fast, rigorous and efficient conformational sampling of biomolecules: Advances in accelerated molecular dynamics ☆

Urmi Doshi, Donald Hamelberg *

Department of Chemistry and the Center for Biotechnology and Drug Design, Georgia State University, Atlanta, GA 30302-3965, United States

ARTICLE INFO

Article history:
Received 18 June 2014
Received in revised form 12 August 2014
Accepted 13 August 2014
Available online 19 August 2014

Keywords:
Accelerated molecular dynamics
Enhanced sampling
Protein folding
Trp-cage
Villin headpiece
Chignolin

ABSTRACT

Background: Accelerated molecular dynamics (aMD) has been proven to be a powerful biasing method for enhanced sampling of biomolecular conformations on general-purpose computational platforms. Biologically important long timescale events that are beyond the reach of standard molecular dynamics can be accessed without losing the detailed atomistic description of the system in aMD. Over other biasing methods, aMD offers the advantages of tuning the level of acceleration to access the desired timescale without any advance knowledge of the reaction coordinate.
Scope of review: Recent advances in the implementation of aMD and its applications to small peptides and biological macromolecules are reviewed here along with a brief account of all the aMD variants introduced in the last decade.
Major conclusions: In comparison to the original implementation of aMD, the recent variant in which all the rotatable dihedral angles are accelerated (RaMD) exhibits faster convergence rates and significant improvement in statistical accuracy of retrieved thermodynamic properties. RaMD in conjunction with accelerating diffusive degrees of freedom, i.e. dual boosting, has been rigorously tested for the most difficult conformational sampling problem, protein folding. It has been shown that RaMD with dual boosting is capable of efficiently sampling multiple folding and unfolding events in small fast folding proteins.
General significance: RaMD with the dual boost approach opens exciting possibilities for sampling multiple timescales in biomolecules. While equilibrium properties can be recovered satisfactorily from aMD-based methods, directly obtaining dynamics and kinetic rates for larger systems presents a future challenge. This article is part of a Special Issue entitled Recent developments of molecular dynamics.

1. Introduction

Current biophysical investigations typically involve monitoring time- and ensemble-averaged properties. For complex biomolecular systems, the interpretation of experimental observations is not always without ambiguity. Lack of microscopic and theoretical models to explain experimental data can lead to the inability to fully understand the physicochemical principles underlying biomolecular function. Computational modeling of biomolecular systems is a powerful tool that complements experiments in providing missing details, helping to verify existing empirical results, predicting new hypotheses and designing new experiments. The success of computational modeling hinges on sufficiently accurate representation of the model and simulation of biologically relevant, long timescales of interest. The spectrum of biomolecular motions is separated by timescales that are over many orders of magnitude. The challenge, therefore, is to preserve the atomic details as well as record short timescale processes while observing slow or rare biological events. At present, atomistic brute-force classical molecular dynamics (MD) implemented on commonly available computational resources is unable to fill this gap. In this regard, implementation of molecular modeling software packages on graphic processing units (GPUs) [1–3], which is speedily replacing central processing units (CPUs) and soon becoming commodity hardware, has made significant impact in accelerating MD calculations. The massively parallel clusters such as Blue Waters and special-purpose supercomputer Anton [4] that are customized for running only MD of biomolecules have provided great opportunity to simulate microsecond to millisecond processes in the conventional manner.

However, access to such resources is currently limited to only a handful of researchers. Another strategy to target the timescale gap has been to develop algorithms that allow enhanced sampling of relevant areas of conformational space and accessing long timescale events, using general-purpose hardware. The objective is to attain enough

☆ This article is part of a Special Issue entitled Recent developments of molecular dynamics.

* Corresponding author at: Department of Chemistry, Georgia State University, P.O. Box 3965, Atlanta, GA 30302-3965, United States. Tel.: +1 404 413 5564; fax: +1 404 413 5505.
E-mail address: dhamelberg@gsu.edu (D. Hamelberg).

http://dx.doi.org/10.1016/j.bbagen.2014.08.003
0304-4165/

sampling, which would then result in Boltzmann distribution of the various conformational states and allow sufficiently accurate calculation of the thermodynamic and, possibly, kinetic properties of the system. Years of efforts in this area have resulted in many notable sampling methods. Some approaches fall under the scheme of modifying the Hamiltonian by adding a bias potential, for example, umbrella sampling [5], local elevation [6], conformational flooding [7], puddle jumping [8], puddle skimming [9], hyperdynamics [10], metadynamics [11], adaptive biasing force method [12] and accelerated MD [13]. The general idea in these methods is to fill up the potential energy minima with a bias so that less computational time is required to move the system out of the minima and evolution of one state to another is faster. In the parallel tempering scheme [14], several copies of the system are initiated at different temperatures or Hamiltonians and configurations sampled in various replicas are allowed to exchange intermittently with the Metropolis criterion to achieve better sampling at the desired condition of low temperature or no bias. As a result canonical ensemble is obtained at each condition of the replicas. Examples under this scheme include replica exchange MD [15], replica exchange with solute tempering [16], integrated tempering MD [17], to name a few. Other approaches include transition path sampling [18], self-guided MD [19], targeted MD [20], milestoning [21], forward flux [22] and finite temperature string methods [23]. The choice of the method depends mainly on the target system and the questions being asked for that system. Each method may be appropriate for a particular problem.

In this paper, we review accelerated MD [13], a Hamiltonian modification method that was introduced almost a decade ago. We refer the readers to another paper that exhaustively reviews accelerated MD, its different implementations and applications [24]. Although here, we briefly describe the method and its variants, we mainly concentrate on the recent advances including improvements in its methodology and summarize its applications to small model peptide systems as well as biological macromolecules.

When large energetic barriers separate energy basins, the transition from one state to the other may be infrequent and the system may spend most of the simulation time in one basin in brute-force MD. In the hyperdynamics scheme [10,25], the potential energy of the basin is raised at all the regions other than the transition state by adding a bias potential. Simulating on the modified potential that effectively has reduced barriers increases the rate of transitions from one basin to the other. The effects of the bias can be corrected subsequently to obtain the original canonical distribution. Based on the transition state theory, the time spent on the modified potential is derived such that it is proportional to the barrier height, and hence is less than that spent on the original unbiased potential. In transition state theory, the rate of escape is estimated from the equilibrium flux across the dividing surface on the foreknown reaction coordinate. Similarly, in certain biased sampling methods, dynamics is performed on a modified potential projected onto a pre-known reaction coordinate or collective set of variables. Unlike these methods, in hyperdynamics the system evolves from one state to another without advance knowledge about the number of states, properties of the states and position of the dividing surface. However, identifying the transition state regions is essential in hyperdynamics so that no bias is added to the saddle regions. The transition state regions are normally identified 'on-the-fly' from the local curvature of the potential energy surface which involves computationally expensive calculation of the eigenvalues of the Hessian matrix of the multi-variable potential energy function, for example, regions where the lowest eigenvalue of the Hessian matrix is negative belong to the saddle point regions. Hyperdynamics is based on the assumption that the system equilibrates in a basin before transitioning out and transition state theory is applicable to the modified potential. Using the transition state theory rate expression, it is shown that under this scheme the relative rates of transitioning to neighboring states are preserved on the modified potential [25]. Several forms [8,26–29] of the bias potential have been proposed; however, their applications have been limited to only small real systems and not sufficiently validated for complex macromolecular biological systems. Moreover, in some cases, the prescribed bias potential does not preserve the shape of the underlying potential energy landscape in the minima, resulting in discontinuous force at the points where the bias potential merges with the original potential [8,9]. Such scenarios may lead to unstable simulations for bigger systems.

2. Accelerated molecular dynamics

Accelerated MD (aMD), which is closely related to hyperdynamics, allows for unconstrained simulation, i.e. not constraining a specific set of degrees of freedom or collective variables, without *a priori* knowledge about the topological features of the potential energy landscape [13]. In aMD, unlike hyperdynamics, identifying transition state regions during the course of the simulation is not required. Therefore, the computationally expensive calculation of the Hessian matrix is avoided, extending the application of aMD to larger and more complex biomolecular systems. The bias potential with two parameters, the boost energy E and tuning parameter α, takes the form: $\Delta V(\mathrm{r}) = \frac{(E-V(\mathrm{r}))^2}{\alpha + E - V(\mathrm{r})}$. E and α are constants that are preset before starting an accelerated MD run. When the potential energy of a system is lower than the boost energy E, simulation is performed on the modified potential, i.e. $V^*(\mathrm{r}) = V(\mathrm{r}) + \Delta V(\mathrm{r})$. At regions where the potential energy is equal to or higher than the threshold energy E, MD is performed on the original unbiased potential. This prescription of $\Delta V(\mathbf{r})$ ensures that the derivative $\frac{dV^*(\mathrm{r})}{d\mathrm{r}}$ is continuous for any value of $V^*(\mathbf{r})$. The computational overhead of aMD as compared to conventional MD is negligible, as calculation of forces, i.e. $F^* = -\nabla V^*(\mathrm{r}) = -\left[\nabla V(\mathrm{r})\left(\frac{\alpha}{\alpha + E - V(\mathrm{r})}\right)^2\right]$ require only an additional computation of the bias potential and the respective scaling factor, $\left(\frac{\alpha}{\alpha + E - V(\mathrm{r})}\right)^2$. Unlike other methods that involve biasing the potential, restricting the phase space and knowing the progress coordinate are not requisites of accelerated MD. How aggressively a system is accelerated depends on the selection of E and α. Shown in Fig. 1 are hypothetical unmodified potential and potentials after adding various levels of bias. When α tends to infinity the modified potential approaches the original potential (blue curve of Fig. 1), whereas when α is set to zero (a condition similar to purple curve of Fig. 1) the modified potential is essentially equivalent to that in the 'puddle skimming' [9] algorithm, i.e. $V^*(\mathbf{r}) = E$ and therefore, flat, and $\frac{dV^*(\mathrm{r})}{d\mathrm{r}} = 0$ at all the regions except the saddle points. Such sudden abrupt increase in the force may potentially blow up the simulation. For accelerating any system, E should be set above V_{min} of the starting structure, where V_{min} is the average potential energy of the system obtained from a short normal unbiased MD subsequent to equilibration. Ideally, E should be set to a value such that the transition state region is above E. In such cases (Fig. 1A), any value of α (except when α is close to zero) will preserve the basic shape of the potential energy surface and fulfill the requirement for reweighting time based on the assumption of transition state theory (i.e. transition state regions are not modified, thus maintaining the proportionality between the ratio of the rates of escaping out of a minima obtained from the unmodified and the modified potentials. Refer to Equation 10 in Ref. [25] for details. If E is set to a very high value, it is possible that $\Delta V^*(\mathbf{r}) \neq 0$ at the saddle point region (the lower barrier in Fig. 1B), preventing direct reweighing of time to obtain the correct time, but does not affect recovery of equilibrium properties. In such cases, retrieval of true kinetics fails (see Section 3). Also, if α is set to zero, the modified potential becomes flat and the system undergoes random walk due to zero force i.e. $-\frac{dV^*(\mathrm{r})}{d\mathrm{r}} = 0$ at most of the regions of the potential energy landscape (Fig. 1B).

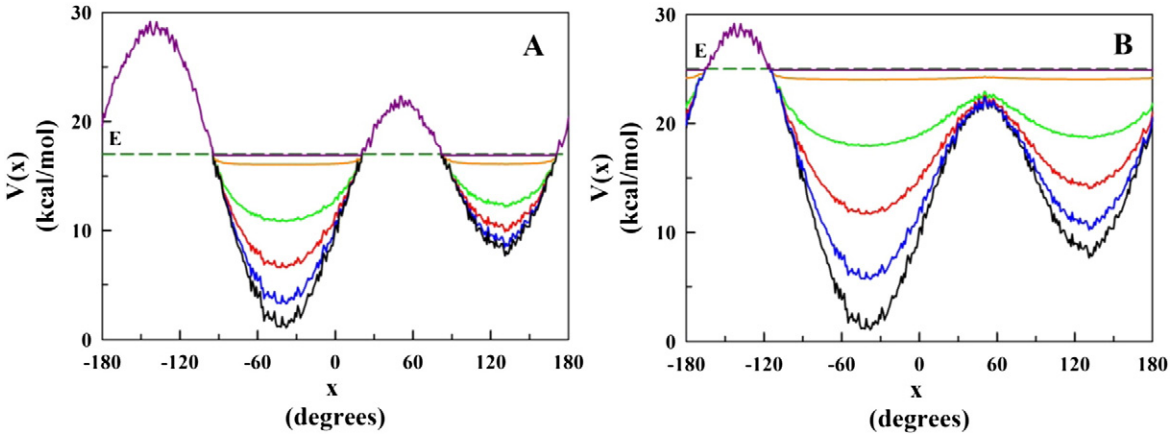

Fig. 1. A schematic representation of accelerated molecular dynamics. The unmodified (black) potential energy surface is projected onto a single dimension *x* (for e.g. a torsional degree of freedom). (A) *E* (dark green dotted line) is set to a lower value such that transition state regions are not modified. (B) *E* is set to a relatively higher value affecting one of the barrier regions. Modified potentials are shown with different levels of $\alpha = 0.1$ (purple), $\alpha = 1$ (orange), $\alpha = 10$ (green), $\alpha = 30$ (red), $\alpha = 100$ (blue).

2.1. Reweighting and retrieval of equilibrium properties

In accelerated MD, reweighting each configuration by the strength of the bias at that position reproduces the correct canonical probability distribution [13]. If $\langle A \rangle$ is an ensemble average of an observable *A* on the original unbiased potential, i.e. $\langle A \rangle = \frac{\int A(\mathrm{r})\, e^{-\beta V(\mathrm{r})} d\mathrm{r}}{\int e^{-\beta V(\mathrm{r})} d\mathrm{r}}$, the ensemble average of *A* on the modified potential is $\langle A^* \rangle = \frac{\int A(\mathrm{r})\, e^{-\beta V^*(\mathrm{r})} d\mathrm{r}}{\int e^{-\beta V^*(\mathrm{r})} d\mathrm{r}}$ which can be corrected to $\langle A \rangle$ by simply multiplying by $e^{\beta \Delta V(\mathbf{r})}$ ($\beta = 1/k_B\mathrm{T}$), i.e. $\langle A \rangle = \frac{\int A(\mathrm{r})\, e^{-\beta V(\mathrm{r}) - \beta \Delta V(\mathrm{r})} e^{\beta \Delta V(\mathrm{r})} d\mathrm{r}}{\int e^{-\beta V(\mathrm{r}) - \beta \Delta V(\mathrm{r})} e^{\beta \Delta V(\mathrm{r})} d\mathrm{r}} = \frac{\int A(\mathrm{r})\, e^{-\beta V^*(\mathrm{r})} e^{\beta \Delta V(\mathrm{r})} d\mathrm{r}}{\int e^{-\beta V^*(\mathrm{r})} e^{\beta \Delta V(\mathrm{r})} d\mathrm{r}} = \frac{\langle A(\mathrm{r}) e^{\beta \Delta V(\mathrm{r})} \rangle_*}{\langle e^{\beta \Delta V(\mathrm{r})} \rangle_*}$. Fig. 2A shows the successful reproduction of the free energy profiles of

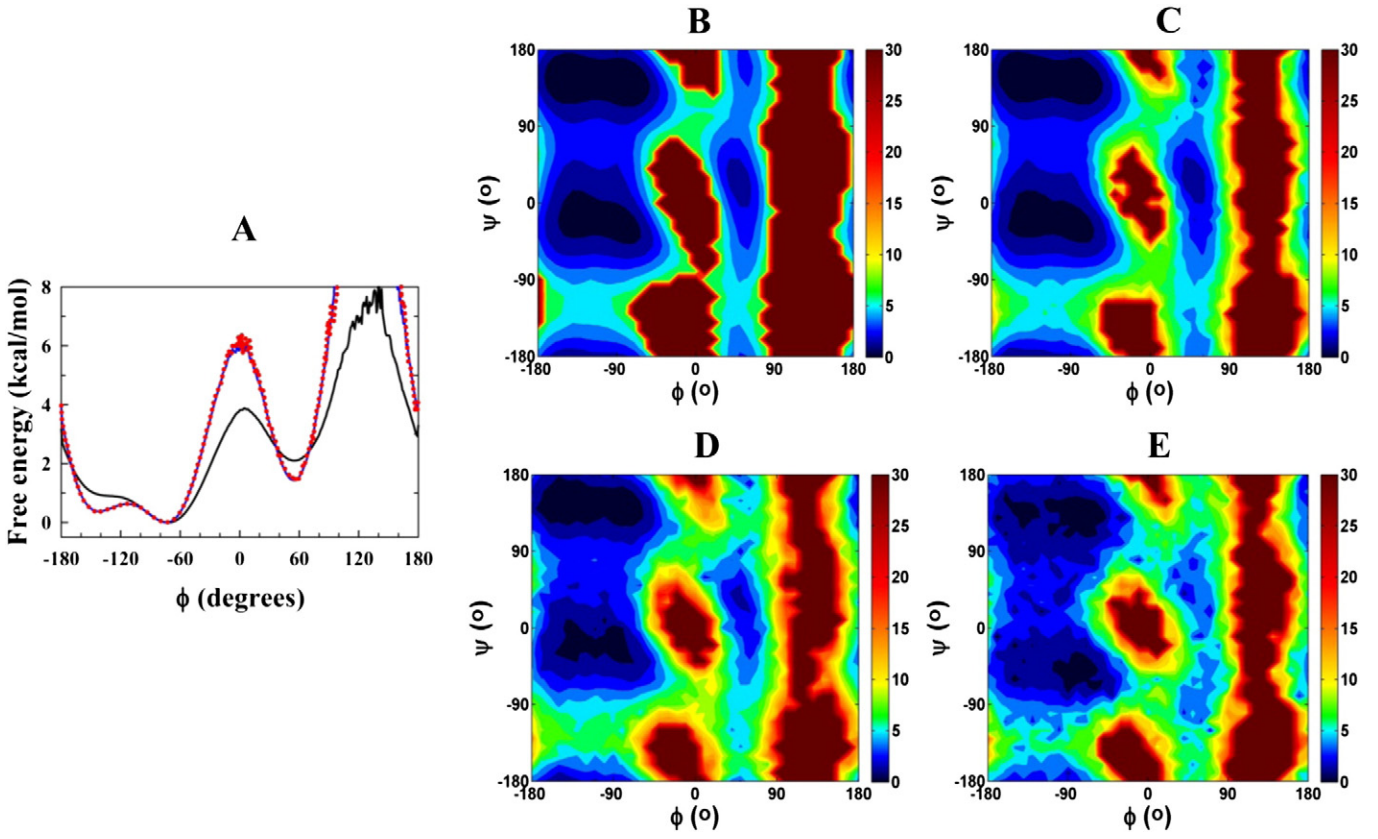

Fig. 2. Comparison of free energy profiles from unbiased and accelerated MD simulations. (A) One-dimensional free energy profiles (FEP) of alanine dipeptide projected on to the backbone ϕ dihedral angle. Shown are the FEPs from the reference normal unbiased (blue), unweighted FEP from aMD (black) and reweighted FEP from aMD (red) simulations. The overlap between the red and blue profiles indicates successful retrieval of correct canonical distribution from aMD. ϕ–ψ free energy contour plots of tryptophan dipeptide obtained from (B) the reference unbiased simulation and aMD using (C) $\alpha = 30$ kcal/mol, (D) $\alpha = 15$ kcal/mol and (E) $\alpha = 10$ kcal/mol. The boost energy is set to the same value in all the three levels of acceleration.

Alanine dipeptide (Ace-Ala-Nme) projected onto the ϕ dihedral angle. The ϕ–ψ free energy plots of tryptophan dipeptide (Ace-Trp-Nme) (Fig. 2B–E) show that all the relevant areas of conformational space observed in conventional MD are sampled in accelerated MD. However, exponential reweighting results in the introduction of statistical errors in the retrieved ensemble properties. A broad distribution of statistical weights and dominance of a few sampled points with high weights reduces the effective sampling size and thus, the precision of the estimated probability distribution (more details in Section 2.2.6). With the increase in the level of acceleration, the deviation of the modified potential from the original potential is larger, resulting in higher statistical errors as evident from the decrease in the smoothness of the contour lines in the ϕ–ψ plots of tryptophan dipeptide (Fig. 2C–E).

A statistical theory has been developed that allows quantitative estimation of statistical error associated with the reduction in the effective number of sampled points due to reweighing [30]. This theory relates the effective and independent (uncorrelated) number of sampled points N^* and the distribution of statistical factors s (where $s = \beta\Delta V(\mathbf{r})$) to the uncertainty ε associated with a sampled region having a relative free energy of ΔF to the most sampled region: $N* \times e^{\frac{-\Delta F_x}{k_B T}} \times \int_{s_l}^{s_h} e^{s-s_h} p(s)ds = \frac{1}{\left(e^{\varepsilon/k_B T}-1\right)^2}$. The magnitude of the uncertainty due to reweighting depends on the number of data points that have statistical factors clustered closely to the highest value s_h. The reduction in the effective sample size will be less if there is relatively large number of data points with weights closer to the highest weight. If the deviation of statistical factors from s_h is larger such that the distribution $p(s)$ is lopsided towards lower s, the reweighting error will be relatively higher (Fig. 3A–C). To reduce statistical errors due to reweighting several variants of aMD have been proposed, as discussed in the next section.

2.2. Variants and implementations of accelerated molecular dynamics

An all-atom force field is typically represented as a potential energy functional, which in its simplest form is given by the summation of the energy terms arising from oscillations around an equilibrium bond length, $V_B(\mathbf{r})$, equilibrium angle, $V_\theta(\mathbf{r})$, torsional rotations, $V_D(\mathbf{r})$, and non-bonded energy terms involving van der Waals interactions, $V_{LJ}(\mathbf{r})$, and pairwise electrostatic interactions, $V_{EE}(\mathbf{r})$.

$$V(\mathrm{r}) = \sum_{bonds} K_r\left(r-r_{eq}\right)^2 + \sum_{angles} K_\theta\left(\theta-\theta_{eq}\right)^2 + \sum_{dihedrals}\sum_{n}\frac{V_n}{2}[1+\cos(n\phi-\gamma)] + \sum_{i<j}\left[\frac{A_{ij}}{R_{ij}^{12}}-\frac{B_{ij}}{R_{ij}^{6}}\right] + \sum_{i<j}\frac{q_i q_j}{\varepsilon R_{ij}}$$

The above equation is rewritten as: $V(\mathrm{r}) = V_B(\mathrm{r}) + V_\theta(\mathrm{r}) + V_D(\mathrm{r}) + V_{LJ}(\mathrm{r}) + V_{EE}(\mathrm{r})$.

In principle, the bias potential can be applied to the total potential energy or any of its contributing terms can be boosted separately. Since the torsional degrees of freedom vary the most when conformational changes take place in biomolecules, only the total dihedral energy and 1–4 non-bonded interaction energy were subjected to acceleration in the original implementation of accelerated MD [13]. In the subsequent versions the boost was applied in different manners.

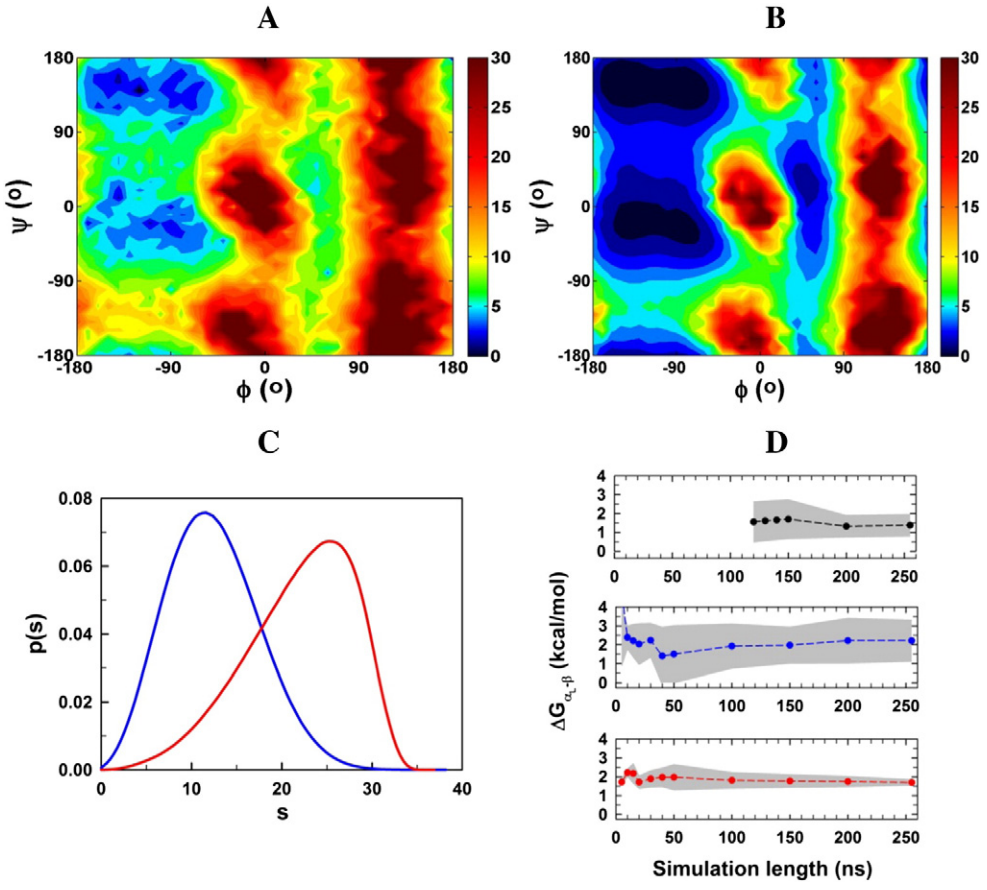

Fig. 3. Comparison of the performance of all-aMD and RaMD. Reweighted free energy profiles of tryptophan dipeptide projected onto the ϕ and the ψ torsions as calculated from (A) all-aMD and (B) RaMD using the same extent of acceleration. (C) Distribution of statistical reweighting factors, s, from all-aMD (blue) and RaMD (red). (D) Free energy difference between extended β-sheet and left-handed α-helical regions as a function of simulation length as calculated from nMD (black), all-aMD (blue) and RaMD (red). Shown are average ΔG values obtained from three independent simulations with their standard deviations (gray areas). Dotted lines are shown to guide the eye.

2.2.1. The dual boost method

In this method, the acceleration is extended to the diffusive degrees of freedom [31,32]. The diffusive motions of the surrounding solvent impede the large-amplitude displacements in biomolecules. Therefore, in this implementation, a boost was added to the dihedral torsions and a separate boost was applied to the total potential, i.e. $V^*(r) = [V_B(r) + V_\theta(r) + [V_D(r) + \Delta V_D(r)] + V_{LJ}(r) + V_{EE}(r)] + \Delta V(r)$, to speed up the diffusion of the water molecules while maintaining the structural properties of water. In this case, the correct canonical ensemble can be recovered by reweighting each frame by the boost factor $exp(\beta[\Delta V_D(\mathbf{r}) + \Delta V(\mathbf{r})])$. This approach has been tested for solvated alanine dipeptide and end-to-end contact formation in a short octapeptide. As compared to conventional MD, the dual boost approach showed faster convergence and more efficient sampling.

2.2.2. Barrier-lowering accelerated MD

In the original implementation of accelerated MD, the conformations in the energy minima experience the largest boost, and thereby, the most unfavorable statistical effects of reweighting. An implementation [33] was proposed to address this issue by redefining the original equation for the bias potential: $\Delta V(r) = \frac{(V(r)-E)^2}{\alpha + V(r)-E}$. In this approach, simulation is performed on the modified potential that has the bias potential subtracted from the original potential energy, i.e. $V^*(r) = V(r) - \Delta V(r)$ when $V(\mathbf{r})$ is greater than the boost energy E and otherwise on the unmodified potential. As a result, the low-energy wells are not affected whereas the magnitude of the barrier heights is reduced. This method has been successfully tested on simple systems such as butane and combined with thermodynamic integration to calculate free energy difference for propane-to-propane transformation. However, for protein systems, this method exhibited a bias towards sampling high energy regions; low energy regions were not adequately sampled. To address this issue, the bias potential was later modified to the following: $\Delta V(r) = \frac{(V(r)-E_1)^2}{(\alpha_1 + V(r)-E_1)\left(1 + e^{\frac{-(E_2 - V(r))}{\alpha_2}}\right)}$. This equation introduces two more parameters, E_2 and α_2 to define the extent of acceleration. The method is referred to as "windowed aMD" [34] as acceleration of the system is allowed in the window between E_1 and E_2 (where E_2 is set higher than E_1). α_1 and α_2 are preset tuning parameters. When $V(\mathbf{r})$ is between E_1 and E_2, the modified potential is $V^*(r) = V(r) - \Delta V(r)$. When $V(\mathbf{r}) < E_1$ or $V(\mathbf{r}) > E_2$, simulation is performed on the original potential. As compared to conventional MD, this method exhibited significantly better sampling in alanine dipeptide and folding of decalanine. Moreover, the method, when incorporated in thermodynamic integration simulations, was also successful in calculating the relative free energy of binding of two peptides to vancomycin.

2.2.3. Replica exchange accelerated MD

The protocol of aMD is versatile, allowing to be combined with other sampling methodologies. In this replica exchange scheme [35], the exchange takes place between Hamiltonians which are simulated with varied boost parameters (E and α) in the original implementation of accelerated MD. Sampling is achieved at all the replicas simulated at different levels of acceleration, including the Hamiltonian with zero bias, i.e. normal MD. Data from such unbiased trajectory need not be reweighted, thus avoiding the exponential reweighting problem of aMD discussed above. Replica exchange aMD has been performed in conjunction with thermodynamic integration and validated in two simple model systems in the gas-phase. This framework has been implemented with the dual boost method and recently with the windowed aMD [36].

2.2.4. Selective accelerated MD

As the name suggests, in selective aMD [37], one can boost only the degrees of freedom that are most relevant for a particular system of interest. The rationale behind selective aMD is to lower the magnitude of statistical weights to reproduce thermodynamic quantities with less statistical inaccuracies due to exponential reweighting. Such selective aMD has been tested for smaller systems such as alanine dipeptide where only the backbone ϕ–ψ dihedral angles were subjected to acceleration as well as for calculation of binding energy using free energy perturbation methods. If the system of interest is large or involving two or more biomolecules, one can choose to accelerate part of the system, for example, boosting only the substrate or the enzyme in an enzyme-substrate complex while simulating the rest of the system with conventional MD [38].

2.2.5. Adaptive accelerated MD

In contrast to raising low-energy minima or lowering barrier regions for the entire potential energy surface as performed in earlier implementations of aMD, in this approach a history-dependent adaptive Gaussian bias potential is applied only to the lowest energy regions [39]. Despite being similar to metadynamics in this respect, i.e. adding Gaussian biasing potentials to potential energy surfaces in a history-dependent fashion, adaptive accelerated MD does not require a predefined set of collective variables. From an aMD run of a specific length of x steps using the boost potential of the original implementation, average principal component projection coordinates are calculated and a two-dimensional Gaussian potential centered at these coordinates is added to the original boost potential. An aMD simulation is carried out for another x steps to determine the principal component projection coordinates as centers for the next Gaussian potential to be added to the previous boost potential. A dual boost adaptive aMD has been performed to sample the various conformations of a substrate-free 404-residue member of the cytochrome-P450 superfamily. Conformations that were not sampled in the standard aMD run were identified by adaptive aMD simulation of the same length. Although around 50 adaptive Gaussian bias potentials were needed to achieve appropriate conformational sampling, the magnitude of the perturbation was much smaller than standard aMD.

2.2.6. Accelerated MD on rotatable dihedrals (RaMD) and RaMD with dual boost

With the increase in the size of the system, the total potential energy increases, requiring a large magnitude of bias to accelerate the system in aMD. This leads to large statistical errors due to exponential reweighting of large and broadly distributed statistical factors. To target this reweighting issue, the strategy has, in general, been towards reducing the magnitude of the bias by selectively boosting certain relevant torsions of choice (Section 2.2.4). However, rather than the magnitude of the statistical factors, the statistical theory mentioned in Section 2.1 suggest that it is important to investigate the nature of their distribution, i.e. how closely the statistical factors are distributed with respect to their highest value (Fig. 3C). In biomolecular conformational changes, most often non-rotatable dihedral angles of the ring systems and improper torsion angles that are responsible for maintaining the planarity do not undergo significant transformations.

It is the alteration in the rotatable dihedral angles that are mainly responsible for bringing about conformational transitions. Therefore, in the RaMD [40] variant of aMD, the boost potential is applied only to the total rotatable torsional potential whereas the other degrees of freedom are simulated on the unmodified original potential. The performance of all-aMD in which all torsions were accelerated was compared to that of RaMD on alanine- and tryptophan-dipeptides. Although the number of torsions boosted was less in RaMD as compared to all-aMD, the distribution of statistical factors was shifted to higher values (Fig. 3C). Due to such a distribution, the proportion of statistical factors that were closer to the highest value was larger, resulting in less loss in the number of sampled points. Consequently, the reweighted thermodynamic quantities were reproduced with improved statistical precision. As can be seen from Fig. 2C–E, the increase in the extent of

acceleration causes the reweighted free energy plots to be rougher due to increased statistical error associated with greater deviation from the original potential. Markedly, the statistical errors were significantly reduced in case of free energy plots calculated from RaMD (Fig. 3A and B). Moreover, it was possible to achieve the same level of accuracy as in all-aMD with significantly reduced simulation lengths in RaMD [40]. To simulate tryptophan dipeptide, the lengths of simulation in RaMD were decreased by 300–1000 times as compared to all-aMD for the levels of acceleration used in the study. Furthermore, in comparison to standard MD and all-aMD, the calculated free energy difference between extended β-sheet and left-handed α-helical regions from RaMD was seen to converge faster and with notably decreased variance (Fig. 3D).

To further test the sampling efficiency of RaMD, it was implemented with the dual boost approach and tested for folding-unfolding of α-helical proteins such as Trp-cage and the double mutant of the C-terminal domain of Villin headpiece; β-haripins such as Chignolin variant and β-hairpin-forming peptide derived from Nuclear factor erythroid 2-related factor 2 in all-atom detail and explicit solvent [41]. The dual boost method utilized in this work was different than the one previously introduced (Section 2.2.1).

The modified potential has the form

$$V^*(\mathrm{r}) = \left[V_B(\mathrm{r}) + V_\theta(\mathrm{r}) + V_{nonRotD}(\mathrm{r}) + V_{\mathrm{ImprD}}(\mathrm{r})\right] + \left[V_{RotD}(\mathrm{r}) + \Delta V_{RotD}(\mathrm{r})\right] + \left[V_{LJ}(\mathrm{r}) + V_{EE}(\mathrm{r}) + \Delta V_{NB}(\mathrm{r})\right]$$

where two separate bias potentials, $\Delta V_{RotD}(\mathbf{r})$ and $\Delta V_{NB}(\mathbf{r})$ are added to the total rotatable torsional potential and the nonbonded interaction potential, respectively. Equilibrium properties on the original potential can be retrieved by reweighting each configuration by $\beta[\Delta V_{RotD}(\mathbf{r}) + \Delta V_{NB}(\mathbf{r})]$. Starting from completely extended chains, the RaMD-dual boost (db) method was successful in folding the small α-helical proteins and β-hairpins to their correct folded structure (Figs. 4 and 5). In case of Trp-cage, a standard MD trajectory of almost equal length than that of RaMD-db was unable to reach the native structure. Multiple folding-unfolding events were observed (Figs. 4A and 5) in RaMD-db trajectories of these fast folding proteins. Two-dimensional reweighted free energy plots projected onto various local and global collective variables exhibited features that were consistent with previous simulation and experimental studies (Fig. 4C). As compared to folding time of Trp-cage calculated from conventional MD simulations on Anton, RaMD-

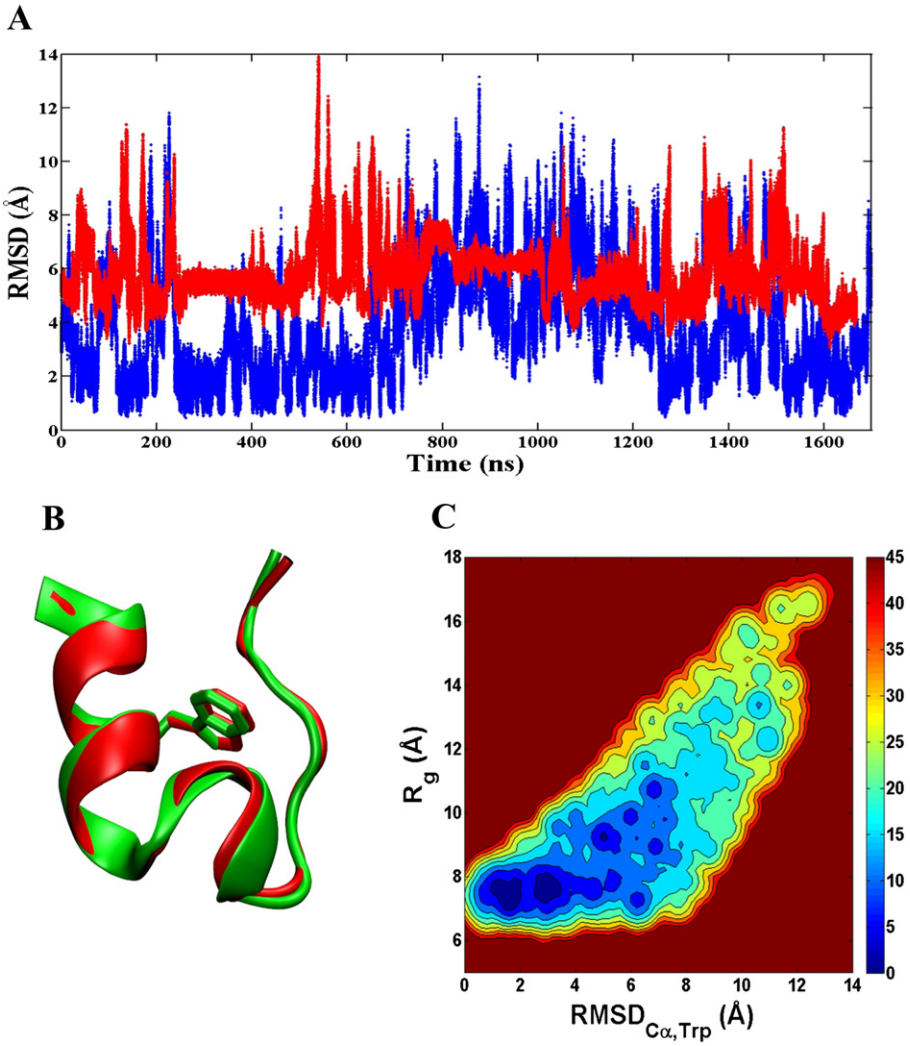

Fig. 4. Folding of Trp-cage with conventional MD and RaMD-db methods. (A) Time series of $RMSD_{Cα,Trp}$ from normal MD (red) and RaMD-db (blue) trajectories of 1.7 μs. Starting from a fully extended structure, Trp-cage was not seen to fold (i.e. RMSD reaching < 2 Å) in the normal MD trajectory, whereas multiple folding-unfolding transitions were observed in a RaMD-db trajectory of almost equal length. (B) Trp-cage structure folded by RaMD-db (red) with root mean square deviation (RMSD) of 0.45 Å with its experimental reference structure (first model of PDB ID: 1L2Y) (green). (C) Reweighted 2-D free energy profile of Trp-cage obtained from RaMD-db simulation is projected onto RMSD and radius of gyration (R_g). For RMSD calculations, Cα atoms of all the residues and heavy atoms of Trp6 side chain are considered. R_g is calculated using all the Trp-cage atoms.

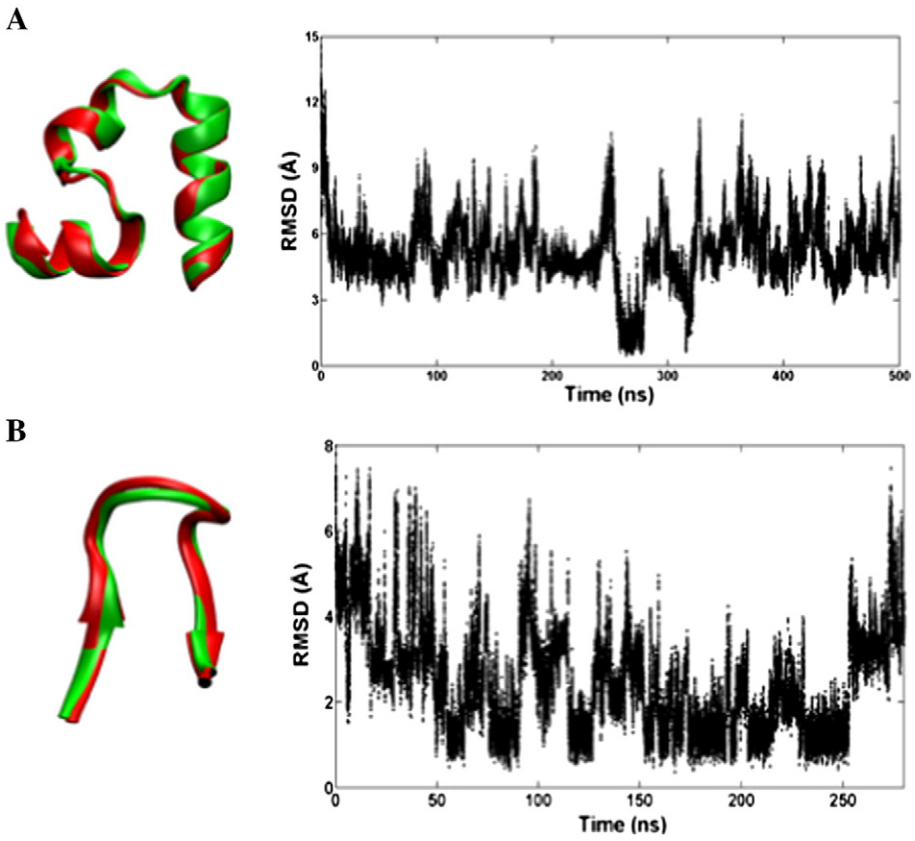

Fig. 5. Folding of Villin headpiece and Chignolin β-hairpin. Folded (red) structures of (A) Villin headpiece-Nle/Nle and (B) β-hairpin forming peptide Chignolin are shown superimposed on their respective native reference (green) PDB structures, i.e. PDB ID: 2F4K and PDB ID: 1UAO, with C-α RMSD of 0.46 and 0.36 Å, respectively. Respective time series of C-α RMSD are shown on the right panel. In case of Villin residues 4–32 were included in RMSD calculations. Residues 1 and 10 were modified to Tyr in the reference structure 1UAO before calculating C-α RMSD.

dual boost method obtained a 180 time-speedup in the folding time for the level of acceleration used in this study. Boosting rotatable dihedrals positively affected the speed of formation of local interactions in both α-helical proteins and β-hairpins. When a bias potential is added to the non-bonded interaction energy, the diffusive motions are sped up, thus helping the formation of nonlocal interactions in β-hairpins and three-dimensional arrangement of secondary structures in proteins. Such rigorous testing on folding of proteins with different secondary structures suggested RaMD-db to be a robust and efficient enhanced sampling method.

2.2.7. Ab initio accelerated MD

In *ab initio* MD, interatomic forces are determined on the fly from first principles electronic structure calculations and not from empirically derived potential with several adjustable parameters. However, in systems with large barriers, the sampling capability of *ab initio* MD is limited. *Ab initio* aMD [42] combines the accurate calculation of free energy with the sampling efficiency of aMD. This method has been preliminarily tested on the microsecond-timescale ring-flipping process in cyclohexane, sampling in bulk water and dissociation of NaCl in water using Car-Parrinello MD [43]. Although, the method suffers from convergence issues in condensed matter systems, convergence was four times faster when *ab initio* aMD was combined with constrained MD as compared to standard constrained MD.

2.2.8. Multidimensional replica exchange accelerated MD

Very recently, an enhanced sampling method has been proposed within the replica exchange (REX) framework that utilizes the strength of statistical mechanical sampling of Hamiltonian aMD in one dimension in conjunction with temperature REX on the second dimension [44]. Temperature REX avoids the statistical errors arising due to reweighting. This method was tested for sampling RNA tetranucleotide and its performance was compared with Hamiltonian REX aMD. Multidimensional REX aMD could sample certain conformations multiple times whereas Hamiltonian REX aMD rarely sampled them. This study showed that boosting torsional energy does not always guarantee appropriate sampling, the exchanges on the temperature dimension help to visit rare conformations. Despite the relatively small size of the model system, a total of 192 replicas (8 replicas of Hamiltonian REX aMD and 24 replicas along the temperature dimension) were used in this study. Sampling a larger biomolecular system would require sizable number of replicas, translating into significant (preferably massively parallel) computational resources. And currently, such resources are not commonly accessible, thus limiting the usage of an otherwise promising method. We recommend an alternative approach in which two-dimensional Hamiltonian REX can be carried out with RaMD combined with the dual boost method (as described in Section 2.2.6). Such a setup would significantly reduce the number of replicas and provide improved sampling due to dual boosting in two dimensions.

2.2.9. Implementations of accelerated MD

aMD and its variants have been implemented in leading simulation packages of AMBER [45] as well as in NAMD [46]. These implementations were in conjunction with non-polarizable fixed-charged force fields. As mentioned in Section 2.2.7, aMD has also been combined with *ab initio* MD methods such as Car-Parrinello MD [42]. Recently, aMD has been implemented for a polarizable force field AMOEBA [47] (Atomic Multipole Optimized Energetics for Biomolecular Applications) on the OpenMM platform that allows faster computing in the GPU environment [48].

3. Retrieval of kinetic properties from accelerated MD

Majority of the studies with aMD have shown that post-simulation reweighting of aMD trajectories can reproduce the correct canonical equilibrium properties. Studies on retrieval of kinetic properties from aMD have been limited. Under the hyperdynamics and aMD scheme, the time the system spends in an energy well before escaping into a neighboring one accumulates as a statistical property such that the time for an accelerated event can be reweighted by the boost factor [10,13], i.e. $t^* = t_{MD}\langle e^{\beta(\Delta V(r(t)))}\rangle$. The actual time taken for the accelerated event to take place on the modified surface is $t_{MD} = N\Delta t$, where N is the number of time steps and Δt is the time step of an MD simulation. The individual time step on the modified potential advances non-linearly as $\Delta t_i^* = \Delta t\ e^{\beta(\Delta V(r(t_i)))}$. The derivation of the reweighted time is based on transition state theory with the assumption that the condition of $\Delta V^*(\mathbf{r}) = 0$ at the saddle point region is fulfilled. However, in practice, for biomolecules with multidimensional landscape, this condition is easy to violate, thereby, failing to reproduce original kinetics by time reweighting. Using a model system for cis–trans isomerization, i.e. *N*-methyl acetylamide, it has been shown that when $\Delta V^*(\mathbf{r}) \neq 0$ at the transition state due to the choice of the acceleration parameters, time reweighting no longer reproduces correct kinetics [49] (Fig. 6B).

When a lower boost is applied that ensures that the transition state regions are not modified by the addition of the bias potential, time reweighting regains the true kinetics of the system on the original potential (Fig. 6A). For biomolecules, choosing the appropriate acceleration parameters that strictly gives zero boost at transition state regions for retrieval of kinetics is not trivial, but not impossible. An alternative method has also been suggested that by-passes time reweighting and utilizes Kramers' rate theory in combination with a couple of aMD runs to obtain correct kinetics [49]. From a series of aMD runs in which the boost energy E is kept constant and the tuning parameter α is varied, the actual dynamics on the modified potentials are recorded and the kinetic rates are computed. Also, the free energy profiles from these aMD runs are generated. Using Kramers' framework in the overdamped limit, i.e. $k = (\omega_0\omega_b D_{\alpha,eff}/2\pi k_B T)exp\left(-\Delta G_\alpha{}^{\#}/k_B T\right)$ the true rates are extrapolated to condition of zero bias, i.e. when α tend to infinity. ω_o and ω_b are the curvatures of the well and the barrier regions, respectively, $\Delta G^{\#}{}_\alpha$ is the free energy barrier height and $D_{\alpha,eff}$ is the effective diffusion coefficient on a one-dimensional free energy profile obtained from aMD using a particular value of α. Rearranging Kramers' rate equation and expressing in the log form gives: $\ln(k/\omega_0\omega_b) = \ln(D_{\alpha,eff}/2\pi k_B T) - \Delta G_\alpha{}^{\#}/k_B T$. $\Delta G^{\#}{}_\alpha$ is related to the free energy barrier height from unbiased (i.e. reweighted) simulation, $\Delta G^{\#}{}_0$ by $\Delta G_\alpha{}^{\#} = \Delta G_0{}^{\#} - q/(\alpha + b)$ where q and b are fitting parameters. Normal rate constants can then be obtained from the intercept of the linear fits of $\ln(k/\omega_0\omega_b)$ vs. $q/(\alpha + b)$ and the features of the reweighted one-dimensional free energy profile (Fig. 6C and D). This method has been validated for cis–trans isomerization in the model system in the absence of solvent thus, permitting long unbiased

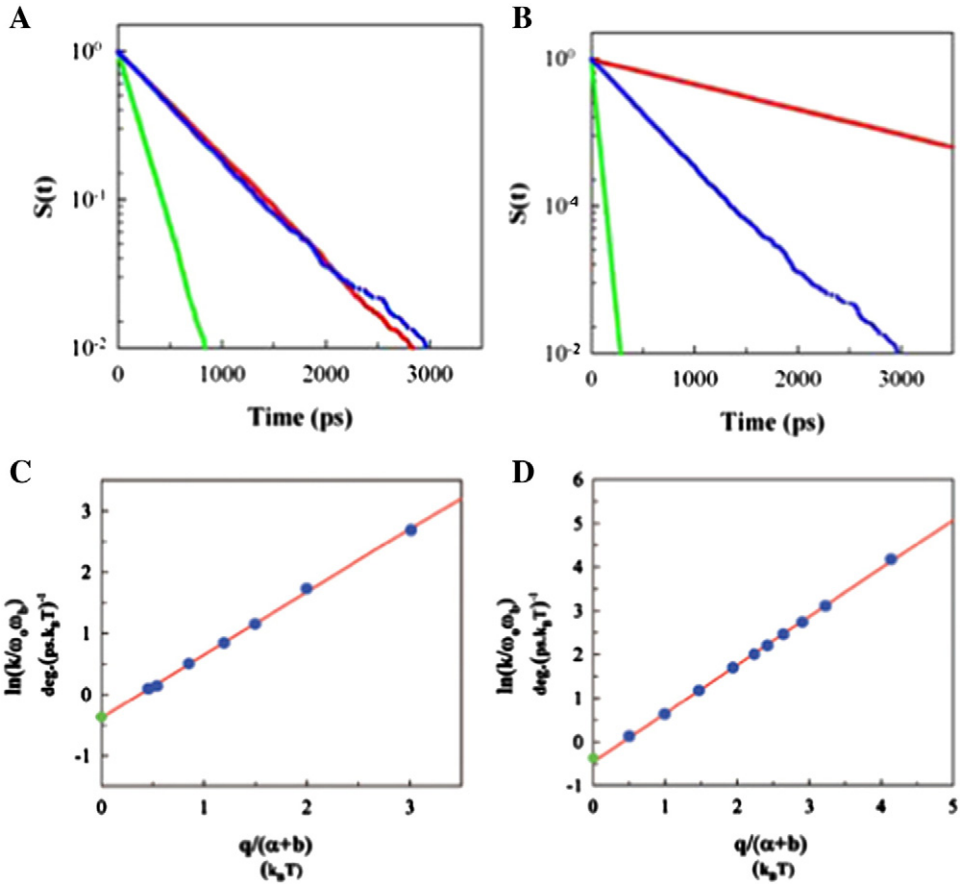

Fig. 6. Retrieval of cis–trans isomerization kinetics on the unbiased potential from accelerated molecular dynamics. Cis–trans isomerization of the ω dihedral angle in *N*-methyl acetamide was simulated with conventional MD and aMD. Decay of probability of survival in the cis well as a function of time was calculated from aMD (green), normal MD (blue) and aMD after reweighting time (red). (A) E was set to a lower value similar to the scenario of Fig. 1A, such that transition state regions between the *cis* and *trans* wells are not modified. (B) E was set to a higher value similar to the scenario depicted in Fig. 1B. Linear plots of $\ln(k/\omega_0\omega_b)$ vs. $q/(\alpha + b)$ (blue filled circles) obtained from several aMD runs are shown in (C) and (D) for conditions corresponding to (A) and (B), respectively. Normal rate constants (green filled circle) can be obtained from the intercept of the linear fits (red solid lines) and features of the reweighted one-dimensional free energy profile, irrespective of whether the bias potential is zero or not at the transition state regions.

simulations to calculate the reference kinetic rates. The rates obtained from the Kramers' approach have been found to be in close agreement with those calculated from unbiased simulations. This method has also been applied to calculate true cis-trans isomerization rates of protein-like peptide as well such as glycyl-prolyl dipeptide in explicit water [50]. Remarkably, the calculated rates were within an order of magnitude of experimental estimates, providing further support for this method.

While Kramers' approach is promising in retrieving unbiased kinetics from aMD runs, the drawback of the method entails running at least a couple of aMD runs and estimating of rate constants from extrapolation, which is based on the assumption that a linear relationship between $\ln(k/\omega_0\omega_b)$ and $q/(\alpha + b)$ is always followed. It may be possible that for larger biomolecular systems, the linearity may break down, resulting in inaccurate estimates of normal rate constants.

For well-studied systems in which the reaction coordinates are known, obtaining realistic kinetics by time reweighting still remains simple and attractive. Efforts in the direction of determining a good reaction coordinate for any system of interest will be worthwhile for a full thermodynamic and kinetic characterization of the system using aMD.

4. Applications of accelerated MD and its variants

Due to its ability to sample long timescale and rare events aMD has been employed to characterize native state dynamics on the microsecond–millisecond timescale in a variety of proteins including HIV-1 protease [51], protein GB3 [52], Ubiquitin [53], H-ras [54], IκBα [55], maltose binding protein [56], and peptidyl prolyl cis-trans isomerases such as cyclophilin [57,58] and Pin1 [59]. Very recently, aMD has been used to fold small fast-folding proteins (Section 2.2.6) [41] initiating from fully extended polypeptide chains. In aMD, the level of acceleration can be tuned to obtain the desired rate of conformational sampling in biomolecules. This feature, which is unique to aMD, has allowed successful reproduction of time- and ensemble-averaged experimental NMR observables such as chemical shifts, residual dipolar and scalar J couplings and S^2 order parameters [52,53,55].

aMD has been extensively validated in short peptide model systems for the process of cis–trans isomerization [13,32,60]. Cis–trans isomerization of ω bonds is a very slow process of biological interest, occurring on the second timescale and not possible to simulate by conventional MD. Cis–trans isomerases speed up the reaction to bring it in the biologically relevant timescale of milliseconds. Functional dynamics in cyclophilin (CypA) and phosphorylation-dependent Pin1 have been characterized using aMD. Whether enzyme dynamics plays a role in functional catalysis has been a question of great interest and a rather controversial issue. Using aMD, dynamics in CypA was accelerated and its direct effects on the rate of cis–trans isomerization in its bound substrates were probed. It was concluded that enzyme dynamics is intricately coupled to the reaction dynamics in the substrate [38,58]. Similar conclusions were drawn from studies on Pin1 [59]. Using Kramers' rate theory, it was shown that the actual speed up in the enzymatic rates arose from the decrease in the free energy barrier heights. Conversely, the dynamical effects of the enzyme, which can be incorporated into the diffusion coefficient of the Kramers' rate expression, limit the enzymatic process. aMD allowed atomistic modeling of uncatalyzed and CypA-catalyzed reactions and generation of accurate free energy profiles [38,61]. The decrease in the free energy barriers in the enzyme-catalyzed reaction is brought about by the transition state stabilization by favorable electrostatic interactions and loss of conformational entropy relative to the ground states [58,61].

Moreover, aMD has been applied for re-optimization of AMBER ω peptide bond parameters [62]. Using aMD in explicit solvent, it was discovered that the default AMBER parameters could not reproduce the experimental *cis–trans* equilibria and free energy barrier heights between the *cis* and the *trans* wells. The new set of re-optimized parameters accurately modeled cis–trans isomerization with quantitative agreement with experimental estimates. Furthermore, aMD has been utilized to investigate the fundamental physical features of the potential energy landscape. A relationship between the aMD parameter α and the effective diffusion coefficient has been established that further provides estimate of local energetic roughness of the potential energy surface [63].

5. Limitations of accelerated MD

Estimation of equilibrium and kinetic properties from aMD and its variants depends on exponential reweighting and therefore, is prone to statistical errors. The more aggressively a system is accelerated, the more deviated is the modified potential from the original potential and greater is the statistical error associated with retrieval of equilibrium and kinetic properties. There is a trade-off between the level of accuracy and the extent of acceleration (and thus sampling speed) desired. Like in any other sampling methods, the bias introduced in aMD depends on the system and the questions to be addressed. Advances in the aMD methodology in the RaMD approach has certainly reduced the reweighting errors, however, not completely amended the problem. In principle, like the equilibrium properties, kinetics of rare or slow events can be recovered from aMD by a time reweighting procedure. The success of this procedure, however, depends on knowing a reaction coordinate along which the transition state can be well defined such that no bias is added to the transition state regions. Caution is required for complex biomolecules with hyper dimensional landscapes to determine an optimum reaction coordinate. Therefore, in order to employ the current state of aMD for retrieving kinetic properties, one needs to select the acceleration parameters carefully such that the system is adequately accelerated while maintaining the condition of not modifying the transition state regions.

6. Discussion and concluding remarks

Accurate computational modeling of the hyper-dimensional and complex potential energy surface of biomolecules depends on the accuracy of the force field and the ability to sufficiently sample long timescale events in atomistic details. However, availability of a perfect force field will still not guarantee accurate representation of a biomolecular system unless desired and relevant areas of conformational space are visited ample number of times. This means that one should have a priori knowledge about the potential energy surface even before launching a computational simulation, which by itself contradicts one of its objectives, i.e. to explore biomolecular conformational space without any prior information that can then be validated experimentally. Running a very long simulation will again not guarantee representation of entire desired conformational space. With increasing the length of the simulation, it is possible that one might collect more and more sampling of conformations that equilibrate on a relatively faster timescale and interesting conformations that are visited only through much slower transitions are never observed. In such cases, convergence of fast relaxing properties is achieved, giving the false impression of adequate sampling even when the so-called 'hidden unknown barriers and conformations' are never sampled [64]. Moreover, starting multiple long trajectories with different conformations will also not assure sampling of such unknown conformations and systematic reduction in statistical errors, an issue exemplified by recent studies by Pomès and coworkers [65]. Such scenarios highlight the importance and need for enhanced sampling techniques that have the capability to explore conformational space in an unconstrained manner. Once appropriate sampling is achieved, the problem with the accuracy of the force field can be tackled. Accelerated molecular dynamics has been established to be robust and efficient biased sampling method with the advantage of simulating biomolecular systems without constraints on pre-determined reaction coordinate or pre-chosen collective variables. Along with reasonably facile setup of aMD in leading simulation packages, post-analysis of aMD trajectories to remove the effects of the bias is also

straightforward. Although exponential reweighting in aMD results in loss of statistical accuracy, sampling of certain conformational transitions can be almost impossible with standard MD, for example, peptidyl-prolyl cis–trans isomerization. The recent variant of aMD in which boost is applied only to the rotatable dihedrals (RaMD) significantly improves the accuracy of retrieved unbiased ensemble averaged properties. RaMD in conjunction with the dual boost approach in which the diffusive degrees of freedom are accelerated has shown promising results for the exceptionally difficult sampling problem in protein folding.

While equilibrium properties can be successfully recovered from aMD and its variant methods, reweighting still remains an issue for retrieval of kinetics. Multidimensional replica exchange approach can completely alleviate the reweighting problem; however, as a result of swapping configurations between replicas, calculation of kinetic rate constants becomes very complex, if not impossible. Using Kramers' rate theory in combination with aMD methods has been robust for obtaining correct rate constants for smaller peptides. For these peptides, the reaction coordinate was well defined, allowing sufficiently accurate projection of free energy surface. It is unclear whether this approach may be equally successful for calculation of kinetic properties of larger systems with complex potential energy surface and unobvious reaction coordinate. Rather than relying on extrapolating from conditions of bias to those where bias is absent, tackling the reweighting issue so that correct dynamical and kinetic information can be obtained from a single biased simulation will be a worthwhile future challenge.

Acknowledgments

We acknowledge financial support from Georgia Research Alliance and National Science Foundation (MCB-0953061). We express our thanks to the Department of Chemistry, the Center for Biotechnology and Drug Design and the Information Systems and Technology services at Georgia State University.

References

[1] A.W. Gotz, M.J. Williamson, D. Xu, D. Poole, S. Le Grand, R.C. Walker, Routine microsecond molecular dynamics simulations with AMBER on GPUs. 1. Generalized born, J. Chem. Theory Comput. 8 (2012) 1542–1555.
[2] R. Salomon-Ferrer, A.W. Gotz, D. Poole, S. Le Grand, R.C. Walker, Routine microsecond molecular dynamics simulations with AMBER on GPUs. 2. Explicit solvent particle mesh ewald, J. Chem. Theory Comput. 9 (2013) 3878–3888.
[3] J.E. Stone, D.J. Hardy, I.S. Ufimtsev, K. Schulten, GPU-accelerated molecular modeling coming of age, J. Mol. Graph. Model. 29 (2010) 116–125.
[4] D.E. Shaw, R.O. Dror, J.K. Salmon, J.P. Grossman, K.M. Mackenzie, J.A. Bank, C. Young, M.M. Deneroff, B. Batson, K.J. Bowers, E. Chow, M.P. Eastwood, D.J. Ierardi, J.L. Klepeis, J.S. Kuskin, R.H. Larson, K. Lindorff-Larsen, P. Maragakis, M.A. Moraes, S. Piana, Y.B. Shan, B. Towles, Millisecond-scale molecular dynamics simulations on Anton, Proc. Conf. High Perf. Comput. Networking, Storage and Analysis, 2009.
[5] G.M. Torrie, J.P. Valleau, Nonphysical sampling distributions in Monte Carlo free-energy estimation: umbrella sampling, J. Comput. Phys. 23 (1977) 187–199.
[6] T. Huber, A. Torda, W. Gunsteren, Local elevation: a method for improving the searching properties of molecular dynamics simulation, J. Comput. Aided Mol. Des. 8 (1994) 695–708.
[7] H. Grubmuller, Predicting slow structural transitions in macromolecular systems: conformational flooding, Phys. Rev. E. 52 (1995) 2893–2906 (Statistical physics, plasmas, fluids, and related interdisciplinary topics).
[8] J.A. Rahman, J.C. Tully, Puddle-jumping: a flexible sampling algorithm for rare event systems, Chem. Phys. 285 (2002) 277–287.
[9] J.A. Rahman, J.C. Tully, Puddle-skimming: an efficient sampling of multidimensional configuration space, J. Chem. Phys. 116 (2002) 8750–8760.
[10] A.F. Voter, Hyperdynamics: accelerated molecular dynamics of infrequent events, Phys. Rev. Lett. 78 (1997) 3908–3911.
[11] A. Laio, M. Parrinello, Escaping free-energy minima, Proc. Natl. Acad. Sci. 99 (2002) 12562–12566.
[12] E. Darve, D. Rodríguez-Gómez, A. Pohorille, Adaptive biasing force method for scalar and vector free energy calculations, J. Chem. Phys. 128 (2008).
[13] D. Hamelberg, J. Mongan, J.A. McCammon, Accelerated molecular dynamics: a promising and efficient simulation method for biomolecules, J. Chem. Phys. 120 (2004) 11919–11929.
[14] D.J. Earl, M.W. Deem, Parallel tempering: theory, applications, and new perspectives, Phys. Chem. Chem. Phys. 7 (2005) 3910–3916.
[15] Y. Sugita, Y. Okamoto, Replica-exchange molecular dynamics method for protein folding, Chem. Phys. Lett. 314 (1999) 141–151.
[16] P. Liu, B. Kim, R.A. Friesner, B.J. Berne, Replica exchange with solute tempering: a method for sampling biological systems in explicit water, Proc. Natl. Acad. Sci. 102 (2005) 13749–13754.
[17] Y.Q. Gao, An integrate-over-temperature approach for enhanced sampling, J. Chem. Phys. 128 (2008).
[18] C. Dellago, P.G. Bolhuis, F.S. Csajka, D. Chandler, Transition path sampling and the calculation of rate constants, J. Chem. Phys. 108 (1998) 1964–1977.
[19] X.W. Wu, S.M. Wang, Self-guided molecular dynamics simulation for efficient conformational search, J. Phys. Chem. B 102 (1998) 7238–7250.
[20] J. Schlitter, M. Engels, P. Kruger, E. Jacoby, A. Wollmer, Targeted molecular-dynamics simulation of conformational change—application to the T[–]R transition in insulin, Mol. Simul. 10 (1993) 291.
[21] A.K. Faradjian, R. Elber, Computing time scales from reaction coordinates by milestoning, J. Chem. Phys. 120 (2004) 10880–10889.
[22] R.J. Allen, C. Valeriani, P.R. ten Wolde, Forward flux sampling for rare event simulations, J. Phys. Condens. Matter 21 (2009).
[23] W.E., W. Ren, E. Vanden-Eijnden, Finite temperature string method for the study of rare events†, J. Phys. Chem. B 109 (2005) 6688–6693.
[24] P.R. Markwick, J.A. McCammon, Studying functional dynamics in bio-molecules using accelerated molecular dynamics, Phys. Chem. Chem. Phys. 13 (2011) 20053–20065.
[25] A.F. Voter, A method for accelerating the molecular dynamics simulation of infrequent events, J. Chem. Phys. 106 (1997) 4665–4677.
[26] M.M. Steiner, P.A. Genilloud, J.W. Wilkins, Simple bias potential for boosting molecular dynamics with the hyperdynamics scheme, Phys. Rev. B 57 (1998) 10236–10239.
[27] X.W. Wu, S.M. Wang, Enhancing systematic motion in molecular dynamics simulation, J. Chem. Phys. 110 (1999) 9401–9410.
[28] S. Pal, K.A. Fichthorn, Accelerated molecular dynamics of infrequent events, Chem. Eng. J. 74 (1999) 77–83.
[29] X.G. Gong, J.W. Wilkins, Hyper molecular dynamics with a local bias potential, Phys. Rev. B 59 (1999) 54–57.
[30] T. Shen, D. Hamelberg, A statistical analysis of the precision of reweighting-based simulations, J. Chem. Phys. 129 (2008) 034103.
[31] C.A. de Oliveira, D. Hamelberg, J.A. McCammon, On the application of accelerated molecular dynamics to liquid water simulations, J. Phys. Chem. B 110 (2006) 22695–22701.
[32] D. Hamelberg, C.A. de Oliveira, J.A. McCammon, Sampling of slow diffusive conformational transitions with accelerated molecular dynamics, J. Chem. Phys. 127 (2007) 155102.
[33] C.A. de Oliveira, D. Hamelberg, J.A. McCammon, Coupling accelerated molecular dynamics methods with thermodynamic integration simulations, J. Chem. Theory Comput. 4 (2008) 1516–1525.
[34] W. Sinko, C.A.F. de Oliveira, L.C.T. Pierce, J.A. McCammon, Protecting high energy barriers: a new equation to regulate boost energy in accelerated molecular dynamics simulations, J. Chem. Theory Comput. 8 (2012) 17–23.
[35] M. Fajer, D. Hamelberg, J.A. McCammon, Replica-exchange accelerated molecular dynamics (REXAMD) applied to thermodynamic integration, J. Chem. Theory Comput. 4 (2008) 1565–1569.
[36] M. Arrar, C.A.F. de Oliveira, M. Fajer, W. Sinko, J.A. McCammon, w-REXAMD: a Hamiltonian replica exchange approach to improve free energy calculations for systems with kinetically trapped conformations, J. Chem. Theory Comput. 9 (2013) 18–23.
[37] J. Wereszczynski, J.A. McCammon, Using selectively applied accelerated molecular dynamics to enhance free energy calculations, J. Chem. Theory Comput. 6 (2010) 3285–3292.
[38] U. Doshi, L.C. McGowan, S.T. Ladani, D. Hamelberg, Resolving the complex role of enzyme conformational dynamics in catalytic function, Proc. Natl. Acad. Sci. 109 (2012) 5699–5704.
[39] P.R. Markwick, L.C. Pierce, D.B. Goodin, J.A. McCammon, Adaptive accelerated molecular dynamics (Ad-AMD) revealing the molecular plasticity of P450cam, J. Phys. Chem. Lett. 2 (2011) 158–164.
[40] U. Doshi, D. Hamelberg, Improved statistical sampling and accuracy with accelerated molecular dynamics on rotatable torsions, J. Chem. Theory Comput. 8 (2012) 4004–4012.
[41] U. Doshi, D. Hamelberg, Achieving rigorous accelerated conformational sampling in explicit solvent, J. Phys. Chem. Lett. 5 (2014) 1217–1224.
[42] D. Bucher, L.C. Pierce, J.A. McCammon, P.R. Markwick, On the use of accelerated molecular dynamics to enhance configurational sampling in Ab Initio simulations, J. Chem. Theory Comput. 7 (2011) 890–897.
[43] R. Car, M. Parrinello, Unified approach for molecular dynamics and density-functional theory, Phys. Rev. Lett. 55 (1985) 2471–2474.
[44] D.R. Roe, C. Bergonzo, T.E. Cheatham, Evaluation of enhanced sampling provided by accelerated molecular dynamics with Hamiltonian replica exchange methods, J. Phys. Chem. B 118 (2014) 3543–3552.
[45] D.A. Case, T.A. Darden, T.E. Cheatham, C.L. Simmerling, J. Wang, R.E. Duke, R. Luo, R.C. Walker, W. Zhang, K.M. Merz, B. Roberts, S. Hayik, A. Roitberg, G. Seabra, J. Swails, A.W. Goetz, I. Kolossváry, K.F. Wong, F. Paesani, J. Vanicek, R.M. Wolf, J. Liu, X. Wu, S.R. Brozell, T. Steinbrecher, H. Gohlke, Q. Cai, X. Ye, J. Wang, M.J. Hsieh, G. Cui, D.R. Roe, D.H. Mathews, M.G. Seetin, R. Salomon-Ferrer, C. Sagui, V. Babin, T. Luchko, S. Gusarov, A. Kovalenko, P.A. Kollman, AMBER 12, University of California, San Francisco, 2012.
[46] Y. Wang, C.B. Harrison, K. Schulten, J.A. McCammon, Implementation of accelerated molecular dynamics in NAMD, Comput. Sci. Discov. 4 (2011) 015002.

[47] P.Y. Ren, J.W. Ponder, Consistent treatment of inter- and intramolecular polarization in molecular mechanics calculations, J. Comput. Chem. 23 (2002) 1497–1506.
[48] S. Lindert, D. Bucher, P. Eastman, V. Pande, J.A. McCammon, Accelerated molecular dynamics simulations with the AMOEBA polarizable force field on graphics processing units, J. Chem. Theory Comput. 9 (2013) 4684–4691.
[49] Y. Xin, U. Doshi, D. Hamelberg, Examining the limits of time reweighting and Kramers' rate theory to obtain correct kinetics from accelerated molecular dynamics, J. Chem. Phys. 132 (2010) 224101.
[50] U. Doshi, D. Hamelberg, Extracting realistic kinetics of rare activated processes from accelerated molecular dynamics using Kramers' theory, J. Chem. Theory Comput. 7 (2011) 575–581.
[51] D. Hamelberg, J.A. McCammon, Fast peptidyl cis-trans isomerization within the flexible Gly-rich flaps of HIV-1 protease, J. Am. Chem. Soc. 127 (2005) 13778–13779.
[52] P.R. Markwick, G. Bouvignies, M. Blackledge, Exploring multiple timescale motions in protein GB3 using accelerated molecular dynamics and NMR spectroscopy, J. Am. Chem. Soc. 129 (2007) 4724–4730.
[53] P.R. Markwick, G. Bouvignies, L. Salmon, J.A. McCammon, M. Nilges, M. Blackledge, Toward a unified representation of protein structural dynamics in solution, J. Am. Chem. Soc. 131 (2009) 16968–16975.
[54] B.J. Grant, A.A. Gorfe, J.A. McCammon, Ras conformational switching: simulating nucleotide-dependent conformational transitions with accelerated molecular dynamics, PLoS Comput. Biol. 5 (2009).
[55] P.R. Markwick, C.F. Cervantes, B.L. Abel, E.A. Komives, M. Blackledge, J.A. McCammon, Enhanced conformational space sampling improves the prediction of chemical shifts in proteins, J. Am. Chem. Soc. 132 (2010) 1220–1221.
[56] D. Bucher, B.J. Grant, P.R. Markwick, J.A. McCammon, Accessing a hidden conformation of the maltose binding protein using accelerated molecular dynamics, PLoS Comput. Biol. 7 (2011) e1002034.
[57] D. Hamelberg, J.A. McCammon, Mechanistic insight into the role of transition-state stabilization in cyclophilin A, J. Am. Chem. Soc. 131 (2009) 147–152.
[58] L.C. McGowan, D. Hamelberg, Conformational plasticity of an enzyme during catalysis: intricate coupling between cyclophilin A dynamics and substrate turnover, Biophys. J. 104 (2013) 216–226.
[59] H.A. Velazquez, D. Hamelberg, Conformation-directed catalysis and coupled enzyme-substrate dynamics in Pin1 phosphorylation-dependent cis-trans isomerase, J. Phys. Chem. B 117 (2013) 11509–11517.
[60] D. Hamelberg, T. Shen, J.A. McCammon, Phosphorylation effects on cis/trans isomerization and the backbone conformation of serine-proline motifs: accelerated molecular dynamics analysis, J. Am. Chem. Soc. 127 (2005) 1969–1974.
[61] S.T. Ladani, D. Hamelberg, Entropic and surprisingly small intramolecular polarization effects in the mechanism of cyclophilin A, J. Phys. Chem. B 116 (2012) 10771–10778.
[62] U. Doshi, D. Hamelberg, Reoptimization of the AMBER force field parameters for peptide bond (Omega) torsions using accelerated molecular dynamics, J. Phys. Chem. B 113 (2009) 16590–16595.
[63] D. Hamelberg, T. Shen, J. Andrew McCammon, Relating kinetic rates and local energetic roughness by accelerated molecular-dynamics simulations, J. Chem. Phys. 122 (2005) 241103.
[64] D. Tod, A. Romo, Grossfield, Unknown Unknowns: the Challenge of Systematic and Statistical Error in Molecular Dynamics Simulations, Biophys. J. 106 (2014) 1553–1554.
[65] C. Neale, Jenny C.Y. Hsu, Christopher M. Yip, R. Pomès, Indolicidin Binding Induces Thinning of a Lipid Bilayer, Biophys. J. 106 (2014) L29–L31.